

# The Critical Role of Glutamine Transporter ASCT2 in Parkinson's Disease Progression

Rohit Mantena (✉ [rohit.v.mantena@gmail.com](mailto:rohit.v.mantena@gmail.com))

Bergen County Academies: Bergen County Technical Schools <https://orcid.org/0000-0002-4231-0635>

Donna Leonardi

Bergen County Academies: Bergen County Technical Schools

---

## Research Article

**Keywords:** Parkinson's Disease, Glutathione, Glutamine, Antioxidant, ASCT2, Parkinson's Disease Progression, In Vitro

**Posted Date:** November 30th, 2021

**DOI:** <https://doi.org/10.21203/rs.3.rs-1100901/v1>

**License:** © ⓘ This work is licensed under a Creative Commons Attribution 4.0 International License.

[Read Full License](#)

---

# Abstract

Parkinson's Disease (PD) is the second most common neurodegenerative disease, and it plagues millions of people worldwide. PD presents with the loss of dopaminergic neurons, associated with increased oxidative stress. Glutathione (GSH) is a prominent antioxidant; in PD, however, GSH levels are significantly diminished. A precursor for GSH is the amino acid glutamine, which is converted to glutamate and then to GSH. The carrier for glutamine is a transport membrane protein, named ASCT2, and this protein regulates glutamine uptake. In various forms of cancer, inhibition of ASCT2 has led to oxidative stress-mediated apoptosis.

This research looked to elucidate the role ASCT2 can play in PD progression by using  $\alpha$ -synuclein transfected SH-SY5Y neurons as an *in vitro* model of PD. V-9302 is a competitive inhibitor of ASCT2 and was used to diminish ASCT2 transport and glutamine uptake to examine the *in vitro* hallmarks of PD progression. Increasing V-9302 concentrations (decreased ASCT2 activity) led to lower cell viability, higher ROS levels, and higher  $\alpha$ -synuclein levels. Also, increasing V-9302 concentrations led to a decrease in intracellular glutamine, glutamate, and GSH levels. In addition, a power regression model was generated for each of glutamine, glutamate, and GSH vs  $\alpha$ -synuclein to test the biomarker potential of each of these molecules for PD progression. Each of these molecules fit the regression model extraordinarily.

The findings suggest that inhibition of ASCT2 lead to the heightened hallmarks of PD progression. Future research could examine the exciting therapeutic potential of upregulating ASCT2 on PD progression.

# Introduction

Parkinson's Disease (PD) is one of the most devastating medical conditions the human population faces, as more than 10 million people live with PD and 60,000 people are diagnosed yearly in the United States—with this number rising each year <sup>[1]</sup>. It is the second most common neurodegenerative disease, only following Alzheimer's Disease in terms of prevalence. PD is typically a condition of the elderly, and the hallmark symptoms include motor function deterioration, tremors, bradykinesia, hypokinesia, postural instability, and cognitive decline <sup>[2]</sup>. Symptoms often begin on one side, with stiffness in the limbs when walking. These symptoms eventually transition into the ones listed above as the disease progresses<sup>[1]</sup>. However, Parkinson's Disease typically progresses in proportion to normal aging, so it does not significantly reduce the life span of patients <sup>[3]</sup>.

In terms of pathology, Parkinson's Disease is characterized by the loss of dopaminergic neurons in the Substantia nigra pars compacta (SNpc) <sup>[4]</sup>. The SNpc is one of two parts in the Substantia nigra, a nucleus of neurons in the midbrain. The Substantia nigra is critical in managing motor and reward function using the basal ganglia circuitry. The basal ganglia are responsible for several essential functions such as voluntary movement, planning, emotions, and basic cognitive function <sup>[5]</sup>. This loss of

dopaminergic neurons is likely what leads to the traditional symptoms of Parkinson's Disease, which include the motor function and cognitive decline discussed.

In addition, the presence of Lewy bodies (a form of neurofibrillary tangle) is a major hallmark of PD [6]. Like other neurodegenerative diseases, the Lewy body is an aggregation of a misfolded protein and is thought to lead to the progression of the disease. In PD, this protein is  $\alpha$ -synuclein, which is ordinarily involved in synaptic function, as it serves for synaptic vesicle trafficking and neurotransmitter release [7]. However, when there is a mutation in the SNCA gene, the gene which codes for the  $\alpha$ -synuclein protein, the protein misfolds and becomes insoluble. This insoluble  $\alpha$ -synuclein begins to aggregate and forms dense inclusions (Lewy bodies) within the cell. These Lewy bodies are not restricted to the brain, as they can be found throughout the nervous system. They can even extend as far as the spinal cord and the peripheral nervous system.

Oxidative stress is thought to play a major role in Parkinson's Disease pathogenesis, and it is hypothesized that Lewy bodies are one potential avenue through which Reactive Oxygen Species (ROS) form. The ubiquitin-proteasome system (UPS) is the primary pathway in which cells discard waste and damaged proteins. The UPS is used as a defense mechanism during oxidative stress to prevent oxidized proteins from inflicting harm. However, in PD, it is believed that dysfunction in the UPS leads to improper maintenance of ROS and thus, unregulated oxidative stress, as seen in Figure 1. In fact,  $\alpha$ -synuclein, is a substrate of UPS, indicating that there is a link between  $\alpha$ -synuclein/Lewy Bodies and the oxidative stress that forms during Parkinson's Disease [8].

Along with the UPS, excessive levels of dopamine are a major source of ROS formation in the Substantia nigra of PD brains. When dopamine is present in excessive amounts, which is the case for SNpc neurons [9], there is saturation, meaning the excess dopamine cannot be efficiently transported by the vesicular monoamine transporters. Free dopamine is left remaining, and this excess dopamine is readily oxidized to form dopamine quinones, superoxides, and hydrogen peroxide, which contribute to oxidative stress [10]. In various studies, it was found that dopamine quinones formed eumelanin after reacting with neuromelanin [11]. There are several other proposed mechanisms for ROS formation in Parkinson's Disease. For example iron, calcium, and lipids are all molecules that play a role in oxidative stress in the PD brain [8].

Although there are various intracellular antioxidant defense mechanisms, the glutathione (GSH) system is considered to be the most important antioxidant defense system for cellular viability and function maintenance [12]. GSH is a ubiquitous thiol tripeptide which interacts with various ROS, such as hydroxyl radicals, peroxynitrite, and superoxide radicals, and reduces them. GSH is also responsible for reducing any dopamine quinone in the cell that was oxidized from free dopamine. In addition, GSH is important in iron metabolism, as it forms various iron complexes including iron(II)glutathione and the diglutathionyl-dinitrosyl-iron-complexes [13]. It has been shown across multiple studies that diminished levels of GSH leads to elevated levels of oxidative stress in cells. Multiple processes are affected by low levels of GSH,

such as increased oxidative stress in mitochondrial fractions, lipid peroxidation, intracellular calcium, and  $\gamma$ -glutamyl transpeptidase ( $\gamma$ GT) activity <sup>[14]</sup>.

In Parkinson's Disease, it has been established that lower levels of GSH are present in patients. In a study from 1994, researchers found upon postmortem analysis of the CNS that glutathione levels in the substantia nigra of PD patients were reduced by 40% compared to the substantia nigra of similar-age controls. However, this was unique to PD, as patients with other basal ganglia-based neurodegenerative diseases did not experience this drop in GSH levels in the substantia nigra <sup>[15]</sup>.

Glutathione peroxidases (GPXs) are a set of enzymes that reduce hydrogen peroxide, a toxic ROS, into water—utilizing GSH as a reducing agent. It has been found that upregulation of GPX proteins leads to less neuronal loss <sup>[16]</sup>. In dopaminergic neurons in the SNpc, there are overall fewer levels of both GSH and GPX proteins, which provides an explanation as to why this region of the brain is particularly vulnerable to oxidative stress and neurodegeneration.

Glutathione S-transferases (GSTs) are a class of proteins that catalyze glutathione conjugation and are responsible for much of the ROS reduction in the cell. Of the various subtypes of GSTs, the cytosolic forms are predominant in the brain. Because GSTs are vital to the management of intracellular oxidative stress and their levels have been known to be diminished in PD brains, GSTs are a reliable biomarker to track the progression of PD.

GSH is a tripeptide, and its amino acid constituents include cysteine, glutamic acid, and glycine. Glutamine, through the Glutamine/Glutamate cycle, forms glutamate via the enzyme Glutaminase. The glutamate then is eventually synthesized to GSH. Therefore, the levels of glutathione are proportional to the intracellular levels of glutamine, as glutamine is a precursor to glutathione <sup>[17]</sup>. In one study, it was shown that glutamine deprivation increases oxidative stress and decreases GSH levels in a neuroblastoma cell line. Several studies have demonstrated similar results in that reduction of glutamine levels has led to excessive oxidative stress due to not enough GSH being synthesized <sup>[18]</sup>. Therefore, it follows that an increase/decrease in glutamine would lead to modulation of oxidative stress in Parkinson's Disease <sup>[19]</sup>. In fact, certain cancers have been shown to exhibit a “glutamine addiction” in which they significantly increase intracellular glutamine levels as one of their primary means of avoiding apoptosis and preserving cell viability <sup>[18]</sup>.

As seen in Figure 2, glutamine uptake into the cell is mediated by transport protein ASCT2 (also known as SLC1A5). ASCT2 is a 541 amino acid-long membrane transporter protein which belongs to the protein family of Solute Carrier Family 1. Although ASCT2 is responsible for the transport of several amino acids such as asparagine, it primarily functions as a glutamine transporter. The levels of ASCT2 are directly proportional to glutamine uptake and intracellular glutamine levels. In recent years, ASCT2 has become an increasingly popular target for cancer treatment. For numerous *in vitro* cancerous cell lines and even murine *in vivo* models, ASCT2 inhibition and downregulation has led to intrinsic oxidative stress and

apoptosis. The cancer cells were actively using glutamine and converting it into GSH to neutralize the ROS produced from the rapid proliferation and mitochondrial function [18].

Since PD cells (along with other neurodegenerative diseases) have lower levels of GSH—which results in increased oxidative stress—modulating the glutamine levels of the cells could possibly change the levels of oxidative stress accordingly. Similarly, since the amount of ASCT2 is proportional to glutamine uptake, if ASCT2 concentration is increased, oxidative stress theoretically might decrease and if ASCT2 concentration is dropped, oxidative stress should increase. The goal of this research is to potentially identify a functional relationship between the glutamine to glutathione conversion process and PD progression through modulation of the ASCT2 transporter.

To understand the glutamine-glutathione conversion process' role in PD progression, V-9302, a chemical designed to act as a competitive ASCT2 inhibitor [19], was used to limit glutamine uptake into SH-SY5Y cells, transfected to overexpress  $\alpha$ -synuclein. This should in turn worsen PD “progression” in these cells. To assess PD progression in this model, various assays will be performed including cell viability, cell proliferation, Reactive Oxygen Species production, and  $\alpha$ -synuclein quantification. In addition, various hallmarks in the glutamine-glutathione conversion process will be tested, such as glutamine uptake, glutamate levels, and glutathione levels within the cell.

## Materials & Methods

### V-9302 Preparation

V-9302 was purchased from medchemexpress.com (#HY-112683). 1.874 mL DMSO was added to 1 mg V-9302 to form a 1 mM solution. The 1 mM solution was serially diluted to make concentrations 750  $\mu$ M, 500  $\mu$ M, and 250  $\mu$ M. The V-9302 solutions were stored at 4°C. 1  $\mu$ L of solution was added to 100  $\mu$ L of cells in each assay well.

### Cell culture

The SH-SY5Y (human neuroblastoma) cells were provided from ATCC (#CRL-2266). The SHSY5Y cell line was previously transfected to overexpress  $\alpha$ -synuclein using the SNCA plasmid (Cat#RG210606 Origene), exhibiting a 2.1-fold increase in  $\alpha$ -synuclein expression. (Dulbecco's Modified Eagle Medium (DMEM) supplemented with 10% Fetal Bovine Serum and 100 units/ml of penicillin/streptomycin mixture was used for cell culture, and cells were maintained in T75 flasks (Corning, 431464U) at 37°C in 5% CO<sub>2</sub>. When trypsinizing, 0.05% trypsin was used to separate adherent cells from flask walls. For all experiments, cells were seeded at a density of  $1.2 \times 10^5$  cells.

### Cellular Metabolism through ATP Production

SH-SY5Y  $\alpha$ -synuclein-transfected cells were cultured. 100 $\mu$ L of cells were plated in a 96-well plated for 24 hours and then treated with 1 $\mu$ L V-9302 concentrations of 10  $\mu$ M, 7.5  $\mu$ M, 5  $\mu$ M, 2.5  $\mu$ M, 1  $\mu$ M, and 0  $\mu$ M for 48 hours. ATP production was determined using the CellTiter-Glo® Luminescent Cell Viability Assay

#G7570 (Promega Corporation, Madison, WI, USA). CellTiter-Glo® Substrate is mixed with CellTiter-Glo® Buffer and transferred to the CellTiter-Glo® reagent. This solution is then pipetted into the wells, mixed for two minutes, and then incubated for 10 minutes at room temperature, which then measures ATP produced. Then, luminescence is recorded (BioTek ELx808).

## Cell Viability & Photographs

SH-SY5Y  $\alpha$ -synuclein-transfected cells were cultured in T25 flasks (Corning, 431464U). One flask was treated with DMSO and one flask was treated with 7.5  $\mu$ M V-9302, and both were cultured for 48 hours. Cells were photographed at 630X (Nikon Eclipse 80i). Viable and dead cells/mL were measured using trypan blue exclusion assay (ViCell, Beckman Coulter, Indianapolis, IN).

## Cell Proliferation

SH-SY5Y  $\alpha$ -synuclein-transfected cells were cultured. 12000 cells were plated per well in a 96-well plate for 24 hours and then treated with 1  $\mu$ L V-9302 concentrations of 10  $\mu$ M, 7.5  $\mu$ M, 5  $\mu$ M, 2.5  $\mu$ M, 1  $\mu$ M, and 0  $\mu$ M for 48 hours. Cell proliferation was determined using the Celltiter96® Aqueous One Solution #G3582 (Promega Corporation, Madison, WI, USA), according to the manufacturer's protocol. Celltiter96® Aqueous One Solution Reagent was added to the cells and then the plate was incubated at 37°C, 5% CO<sub>2</sub> for 1.5 hours, and then was measured for proliferation levels relative to the amount of NADH produced. The plate was then read for absorbance at 490 nm (BioTek ELx808).

## Intracellular ROS Levels

The SH-SY5Y  $\alpha$ -synuclein-transfected cells were treated with 1  $\mu$ L V-9302 concentrations of 10  $\mu$ M, 7.5  $\mu$ M, 5  $\mu$ M, 2.5  $\mu$ M, 1  $\mu$ M, and 0  $\mu$ M for 42 hours. Cellular oxidative stress was measured by performing the ROS-Glo H<sub>2</sub>O<sub>2</sub> Assay kit (Promega Corporation, Madison, WI, USA) following the manufacturer's protocol. H<sub>2</sub>O<sub>2</sub> Substrate and H<sub>2</sub>O<sub>2</sub> Dilution Buffer were mixed and 20  $\mu$ L of this solution was added to each well and the plate was incubated at 37°C and 5% CO<sub>2</sub> for 6 hours (total of 48 hours treatment time). Then, 100  $\mu$ L of ROS-GLO™ Detection Solution was added to each well and the plate was incubated for 20 minutes at room temperature. Luminescence was measured (BioTek ELx808).

## Preparation of Lysates

$\alpha$ -Synuclein transfected SH-SY5Y cells were cultured in T25 flasks at 1.2e5 cells/mL in 3mL of media. After treatment for 48h with V-9302 at 0, 2.5, 5, 7.5, and 10  $\mu$ M, cells were trypsinized and centrifuged (7min at 1200rpm). The cell pellets were resuspended in 2mL PBS (Invitrogen) and centrifuged (7min at 1200rpm). Cells were resuspended in 1X lysis buffer #9803 (Cell Signaling Technology, Danvers, MA) supplemented with protease inhibitor #P8340 (Sigma) at 1x10<sup>6</sup> cells per 1mL solution. Samples were placed on ice for 10min and then centrifuged (15min at 13,000rpm at 4°C). Lysates were collected and stored at -80°C.

*$\alpha$ -Synuclein Indirect ELISA*

100µL lysate samples in a 96-well ELISA plate were incubated overnight at 4°C. The plate was emptied. 300µL 1X BSA Diluent/Blocking Solution (KPL, Gaithersburg, MD) was used to block wells. A rabbit anti-human primary antibody (1:300) against  $\alpha$ -Synuclein (abcam #ab9443), (Cambridge, MA), was added to wells for 1 hour. After a wash with 1X wash buffer (KPL), a horseradish peroxidase labeled goat anti-rabbit IgG antibody (KPL) (1:300) was added to wells for 1 hour. After a wash (leaving buffer in for 5 minutes), 100µL TMB substrate solution (KPL) was added to wells. Absorbance at 405nm was measured (BioTek ELx808).

## Glutathione ELISA

100µL lysate samples in a 96-well ELISA plate were incubated overnight at 4°C. The plate was emptied. 300µL 1X BSA Diluent/Blocking Solution (KPL, Gaithersburg, MD) was used to block wells. A rabbit anti-human primary antibody (1:300) against GSH (abcam #ab9443), (Cambridge, MA), was added to wells for 1 hour. After a wash with 1X wash buffer (KPL), a horseradish peroxidase labeled goat anti-rabbit IgG antibody (KPL) (1:300) was added to wells for 1 hour. After a wash (leaving buffer in for 5 minutes), 100µL TMB substrate solution (KPL) was added to wells. Absorbance at 405nm was measured (BioTek ELx808).

## Glutathione Levels Assay

The assay kit containing all necessary reagents was purchased from Promega Corp. The SH-SY5Y  $\alpha$ -synuclein-transfected cells were treated with 1µL V-9302 concentrations of 10 µM, 7.5 µM, 5 µM, 2.5 µM, and 0 µM for 48 hours. The assay was carried out according to the manufacturer's instructions. Twenty microliters of Luciferin-NT and 20 µl GST were first mixed with 2 ml GSH-Glo reaction buffer. From this mixture, 10 µl resuspended neuronal samples were mixed with 100 µl GSH reaction buffer containing Luciferin-NT and GST. The mixtures were incubated for 30 min at room temperature. Then 100 µl GSH-Glo reagent were added to each tube followed by 15-min incubation at room temperature. Luminescence was measured and results were analyzed in Microsoft Excel.

## Glutamine Levels

Intracellular concentrations of glutamine were determined using a quantitative colorimetric enzyme assay kit (#EGLN-100; BioAssay Systems, Hayward, CA) according to the manufacturer's protocol. The glutamine assay kit is based on hydrolysis of glutamine to glutamate and colorimetric determination of the product. Glutamine Premix was made by mixing 5µL of 100 mM glutamine solution with 245 µL distilled water and various dilutions were made to establish a standard curve. Enzyme and reagent tubes were reconstituted and working reagent was produced by mixing 65 µL Assay Buffer, 1 µL Enzyme A, 1 µL Enzyme B, 2.5 µL NAD and 14 µL MTT. 80µL of working reagent was added to each well and plate was incubated for 40 minutes at room temperature. 100 µL Stop Reagent was added to each well after incubation and OD at 565 nm was read (BioTek ELx808). Based on the standard curve established, intracellular glutamine concentration was determined.

## Glutamate Levels

The Glutamate-Glo™ assay kit (Promega, J7021) was used to measure intracellular glutamate levels. First, Luciferin Detection Solution was made by combining Reductase, Redutase Substrate, Glutamate Dehydrogenase, and NAD. 50µL of this Luciferin Detection Solution was added to each well and shook for 45 seconds. The plate was incubated at Room Temperature for 1 hour. Luminescence was measured (Biotek ELx808).

## Regression Model

Data generated from previous experiments in this research was utilized to create regression models of Glutamine vs.  $\alpha$ -Synuclein, Glutamate vs.  $\alpha$ -Synuclein, and Glutathione vs.  $\alpha$ -Synuclein. The same concentrations (DMSO, 2.5 µM, 5 µM, 7.5 µM, & 10 µM) were used to measure Glutamine, Glutamate, and Glutathione, as well as  $\alpha$ -Synuclein. The data points corresponding to each concentration for each of these measurements were matched to create regression models of Glutamine vs.  $\alpha$ -Synuclein, Glutamate vs.  $\alpha$ -Synuclein, and Glutathione vs.  $\alpha$ -Synuclein. A power regression was chosen and the  $R^2$  value of each graph was calculated.

## Statistical Analysis

Assays were conducted multiple times with 3 to 5 biological replicates. T-Tests for statistical significance were used with the alpha set at 0.05. Bars on graphs represent STDEV. Diagrams were created using the BioRender Application.

## Results And Discussion

### I. Relationship between V-9302 concentrations and **Glutamine-GSH Conversion Process**

It was first necessary to establish that the blocking of ASCT2 impairs the Glutamine-Glutathione conversion process as expected. Based on figure 3 (and as demonstrated in Figure 7), it is clear that glutamine levels drop as a result of increased V-9302 concentrations. As discussed, V-9302 is a competitive inhibitor of ASCT2, and so the uptake of glutamine is negatively correlated to the levels of V-9302.

In figure 4, (and as demonstrated in Figure 8) the effects of increasing V-9302 concentration on glutamate levels are shown. As seen, glutamate levels significantly decreased as V-9302 concentrations increased. Similar to glutamine, glutamate levels and V-9302 concentrations are inversely related. Although ASCT2 does not act as a carrier for glutamate, glutamine is converted to glutamate via glutaminase, meaning glutamine and glutamate levels are proportional. This glutamine to glutamate conversion via glutaminase is the second step of the glutamine-glutathione conversion process, and it is clear that decreasing ASCT2 activity controls this process.

Figures 5 & 6 (and as demonstrated in Figure 9) display intracellular glutathione levels in response to increasing V-9302 levels. As discussed, in the glutamine-glutathione conversion process, the final step is glutamate being converted to GSH. Just as ASCT2 activity was shown to be directly linked to intracellular glutamine and glutamate levels, GSH levels are thought to be dependent upon ASCT2 activity in PD. As V-

9302 concentrations increase and more ASCT2 transport proteins are inhibited, less GSH is produced in the cell. In Figure 5, because GSH is a ubiquitous thiol tripeptide, a two-step indirect ELISA was performed to assess intracellular levels of GSH. In Figure 6, the luminescent-based assay GSH-GLO was performed to also assess intracellular GSH levels. In both cases, it was found that, as hypothesized, increasing concentrations of V-9302 lead to diminished GSH levels. This finding is critical to understanding the potential of ASCT2 as a regulator of PD progression. Because low GSH levels have consistently been associated with increased PD progression, it is important that decreased ASCT2 seems to have a similar effect on one of the key oxidative stress regulatory mechanisms in the cell. This is a novel finding that ASCT2 levels directly control the GSH levels in a PD model.

## **II. Relationship between V-9302 concentrations and cellular proliferation**

Figure 10 displays how increased V-9302 concentrations lead to a significant decrease in cell proliferation. In PD-affected neurons, cell proliferation is lowered due to an increase in oxidative stress damaging the neurons' mitotic machinery and killing the cells before they can divide. As V-9302 concentrations increase, intracellular glutamine and GSH concentrations drop, as shown in Figures 3, 5, & 6, likely leading to more ROS production. The MTS assay used in this research (Cell-Titer 96®) measures the quantity of formazan product, which is indicative of the cell's ability to proliferate. Oxidative stress as a result of diminished antioxidant levels (including lower concentrations of GSH) kills and damages the neural precursor cells in the sub granular zones of PD brains, so cell proliferation decreases.

### **III. Relationship between V-9302 concentration and Cell Viability**

Figure 11 displays a significant drop in cell viability from DMSO-treated cells to 7.5  $\mu$ M V-9302 treated cells. This is likely due to increased ROS due to a lack of intracellular glutathione, meaning more cells undergo ROS-mediated intrinsic apoptosis. As can be seen from Figures 12 & 13, there is significantly more branching and neuronal presence in the control neurons as opposed to the V-9302 neurons. Due to the same reason as Figure 11, the presence of less glutathione in the V-9302 treated cells leads to more apoptosis and thus less neurons in the photo in Figure 13. Less connections are being formed, and this is representative of PD progression worsening, as in PD, there are less connections being formed and more apoptosis among the neurons.

### **IV. Relationship between V-9302 concentrations and cellular metabolism**

As seen in Figure 14, increased concentrations of V-9302 lead to a significant decrease in cell viability. Cell metabolism is a marker of PD progression; as PD progression accelerates, cell metabolism is decreased. With increasing V-9302 concentrations, more ASCT2 transporters are competitively inhibited, and thus, overall glutamine uptake is reduced. This leads to a loss in GSH antioxidant systems and so the higher oxidative stress is leading to less cell viability. The MTT (Cell-Titer GLO®) assay used quantifies cell metabolism through measurement of ATP levels, which are only present at high quantities in viable,

healthy cells. The excessive ROS produced at high concentrations of V-9302 increases SH-SY5Y death, thereby stunting ATP production and worsening PD progression.

## V. Relationship between V-9302 concentrations and $\alpha$ -Synuclein Levels

In Figure 15, it is clear that an increase of V-9302 concentrations correlates with an increase in  $\alpha$ -Synuclein levels. A two step indirect ELISA was performed to assess the levels of  $\alpha$ -Synuclein in the SH-SY5Y  $\alpha$ -Synuclein- transfected cells treated with V-9302. As can be seen,  $\alpha$ -Synuclein levels significantly increase in the presence of increased levels of V-9302. This agrees with the literature which states that increased ROS exacerbates  $\alpha$ -Synuclein production in neurons. Therefore, this provides further evidence of the link between ASCT2 activity and PD progression.

## VI. Relationship between V-9302 concentrations and ROS Levels

As can be seen from figure 16, increasing V-9302 concentrations significantly increase intracellular ROS levels. Just as hypothesized, the decreased ASCT2 activity as a result of V-9302 inhibition leads to less glutamine uptake. Glutamine is then not converted to glutamate which is then not converted to glutathione, leading to an increased presence of ROS. As discussed, GSH reduces  $H_2O_2$  levels in conjunction with Glutathione Peroxidases (GPXs). The assay used to assess intracellular levels was the ROS-GLO kit that measures intracellular  $H_2O_2$ , and as less glutathione was available,  $H_2O_2$  increased with higher V-9302 concentrations. These increased levels of  $H_2O_2$  lead to more neuronal death and dysfunction, thereby worsening PD progression. Again, through this mechanism, there is further evidence that ASCT2 has the potential to modify PD progression.

## VII. Regression Models Showing Biomarker Potential of Glutamine, Glutamate, Glutathione in PD Model

After plotting the three graphs, Glutamine vs.  $\alpha$ -Synuclein, Glutamate vs.  $\alpha$ -Synuclein, and Glutathione vs.  $\alpha$ -Synuclein, and analyzing the coefficient of determinations, it is apparent that all three steps of the Glutamine-Glutathione conversion process can be viewed as biomarkers of  $\alpha$ -Synuclein production in this *in vitro* model. For Glutamine vs.  $\alpha$ -Synuclein (Figure 17), the coefficient of determination is 0.9186, which is very high. This indicates that a power regression fit of the data can be reliably used to predict  $\alpha$ -Synuclein levels (percent control) when given the Glutamine uptake (percent control).

For Glutamate vs  $\alpha$ -Synuclein (Figure 18), the coefficient of determination was 0.8993. This is still a high  $R^2$  and supports the idea that glutamate levels can be used as a biomarker of  $\alpha$ -Synuclein production, but it is lower than Glutamine. This could be because glutamate is an amino acid that is produced and taken into the cell through other means, not just by being converted from glutamine to glutamate via glutaminase.

For Glutathione vs.  $\alpha$ -Synuclein (Figure 19), the coefficient of determination was 0.9161, which is just below glutamine. Again, 0.9161 is a very high  $R^2$ , so Glutathione levels can be used as a reliable

biomarker of  $\alpha$ -Synuclein production.

When comparing the three steps of the conversion process, it is apparent that, while all have very high  $R^2$  values, Glutamine & Glutathione are the best biomarkers to measure  $\alpha$ -Synuclein production and PD progression in this *in vitro* model. Like mentioned, Glutamate likely has a lower coefficient of determination because there are methods in the cell to uptake Glutamate and produce Glutamate, as Glutamate is a vital amino acid and neurotransmitter for synaptic transmission.

## Conclusion

In all, it is evident that ASCT2 displays a significant role in Parkinson's Disease progression through the controlling of the glutamine to glutathione conversion process. As discussed, PD progression is directly correlated to Reactive Oxygen Species levels, and as ROS levels increase, PD progression worsens. In fact, neuronal death and dysfunction across all neurodegenerative diseases—including PD—is caused by ROS-mediated intrinsic apoptosis. In addition, diminished levels of glutathione have been strongly associated with increased neurodegeneration, which indicates that levels of GSH and its precursor glutamine should be at the forefront of targets for stopping PD progression.

In this research, an association between ASCT2 activity and PD progression in an *in vitro* model of PD (SH-SY5Y–  $\alpha$ -synuclein transfected neurons) has been established. The results have demonstrated that as levels of V-9302 increase and ASCT2 activity decreases, the glutamine-glutathione conversion process is diminished, as evidenced by the decreased glutamine uptake, glutamate levels, and GSH levels. In addition, decreased ASCT2 leads to worsened PD progression in this model, as evidenced by decreasing cell viability, decreasing cell proliferation, increasing ROS levels, and increasing  $\alpha$ -synuclein levels. Finally, the power regression models generated that modeled the relationships between parts of the glutamine-glutathione conversion process and  $\alpha$ -synuclein production indicate that ASCT2 can significantly alter PD progression in this *in vitro* model.

Future studies can directly upregulate ASCT2 or modulate various transcription factors to increase ASCT2 levels and examine the effects on PD progression. Due to the COVID-19 pandemic and the resulting lab shutdowns and delayed delivery times, the materials necessary to upregulate ASCT2 expression and study the effects on PD were not able to be purchased. Furthermore, the relationship between ASCT2 and PD progression can be studied *in vivo* to achieve a more representative understanding of this potential key association.

## Declarations

### Acknowledgements

The completion of this research would not have been possible without the gracious support and mentorship from my mentor, Mrs. Donna Leonardi. I also appreciate the Bergen County Academies institution and the Cell Biology Lab for providing me with funding and the space to perform this research.

## Ethics Approval

Not applicable

## Consent to Participate

Not applicable

## Consent for Publication

Not applicable

## Funding

*The authors declare that no funds, grants, or other support were received during the preparation of this manuscript.*

## Competing Interests

The authors have no relevant financial or non-financial interests to disclose.

## Author Contributions

All authors contributed to the study conception and design. Material preparation, data collection and analysis were performed by Rohit Mantena. The first draft of the manuscript was written by Rohit Mantena and Donna Leonardi commented on previous versions of the manuscript. All authors read and approved the final manuscript.

## Data Availability

The datasets generated during and analyzed during the current study are not publicly available due to being collected privately, but are available from the corresponding author on reasonable request.].

## References

1. *Statistics*. Parkinson's Foundation. (n.d.). Retrieved September 30, 2021, from <https://www.parkinson.org/Understanding-Parkinsons/Statistics>.
2. Jankovic, J., & Tan, E. K. (2020). Parkinson's disease: etiopathogenesis and treatment. *Journal of Neurology, Neurosurgery, and Psychiatry*. <https://doi.org/10.1136/jnnp-2019-322338>
3. MediLexicon International. (2021, March 9). *Parkinson's life expectancy: Stages and treatment options*. Medical News Today. Retrieved October 16, 2021, from <https://www.medicalnewstoday.com/articles/parkinsons-life-expectancy#summary>.
4. Masato, A., Plotegher, N., Boassa, D., & Bubacco, L. (2019). Impaired dopamine metabolism in parkinson's disease pathogenesis. *Molecular Neurodegeneration*, 14(1).

<https://doi.org/10.1186/s13024-019-0332-6>

5. Sonne, J. (2020, November 8). *Neuroanatomy, substantia nigra*. StatPearls [Internet]. Retrieved September 30, 2021, from <https://www.ncbi.nlm.nih.gov/books/NBK536995/>.
6. Wakabayashi, K., Tanji, K., Odagiri, S., Miki, Y., Mori, F., & Takahashi, H. (2012). The lewy body in parkinson's disease and related neurodegenerative disorders. *Molecular Neurobiology*, *47*(2), 495–508. <https://doi.org/10.1007/s12035-012-8280-y>
7. UniProt ConsortiumEuropean Bioinformatics InstituteProtein Information ResourceSIB Swiss Institute of Bioinformatics. (2021, June 2). *Alpha-Synuclein*. UniProt ConsortiumEuropean Bioinformatics InstituteProtein Information ResourceSIB Swiss Institute of Bioinformatics. Retrieved September 30, 2021, from <https://www.uniprot.org/uniprot/P37840>.
8. Dias, V., Junn, E., & Mouradian, M. M. (2013). The role of oxidative stress in parkinson's disease. *Journal of Parkinson's Disease*, *3*(4), 461–491. <https://doi.org/10.3233/jpd-130230>
9. Chinta, S. J., & Andersen, J. K. (2005). Dopaminergic neurons. *The International Journal of Biochemistry & Cell Biology*, *37*(5), 942–946. <https://doi.org/10.1016/j.biocel.2004.09.009>
10. Segura-Aguilar, J., Paris, I., Muñoz, P., Ferrari, E., Zecca, L., & Zucca, F. A. (2014). Protective and toxic roles of dopamine in parkinson's disease. *Journal of Neurochemistry*, *129*(6), 898–915. <https://doi.org/10.1111/jnc.12686>
11. Carstam, R., Brinck, C., Hindemith-Augustsson, A., Rorsman, H., & Rosengren, E. (1991). The neuromelanin of the human substantia nigra. *Biochimica Et Biophysica Acta (BBA) - Molecular Basis of Disease*, *1097*(2), 152–160. [https://doi.org/10.1016/0925-4439\(91\)90100-n](https://doi.org/10.1016/0925-4439(91)90100-n)
12. Jones, D. P. (2006). Extracellular redox state: Refining the definition of oxidative stress in aging. *Rejuvenation Research*, *9*(2), 169–181. <https://doi.org/10.1089/rej.2006.9.169>
13. Berndt, C., & Lillig, C. H. (2017). Glutathione, glutaredoxins, and iron. *Antioxidants & Redox Signaling*, *27*(15), 1235–1251. <https://doi.org/10.1089/ars.2017.7132>
14. Smeyne, M., & Smeyne, R. J. (2013). Glutathione metabolism and parkinson's disease. *Free Radical Biology and Medicine*, *62*, 13–25. <https://doi.org/10.1016/j.freeradbiomed.2013.05.001>
15. Sian, J., Dexter, D. T., Lees, A. J., Daniel, S., Jenner, P., & Marsden, C. D. (1994). Glutathione-related enzymes in brain in parkinson's disease. *Annals of Neurology*, *36*(3), 356–361. <https://doi.org/10.1002/ana.410360306>
16. Wang, H., Cheng, E., Brooke, S., Chang, P., & Sapolsky, R. (2003). Over-expression of antioxidant enzymes protects cultured hippocampal and cortical neurons from necrotic insults. *Journal of Neurochemistry*, *87*(6), 1527–1534. <https://doi.org/10.1046/j.1471-4159.2003.02123.x>
17. Daye, D., & Wellen, K. E. (2012). Metabolic reprogramming in cancer: Unraveling the role of glutamine in tumorigenesis. *Seminars in Cell & Developmental Biology*, *23*(4), 362–369. <https://doi.org/10.1016/j.semcdb.2012.02.002>
18. Chen, L., & Cui, H. (2015). Targeting glutamine induces apoptosis: A cancer therapy approach. *International Journal of Molecular Sciences*, *16*(9), 22830–22855. <https://doi.org/10.3390/ijms160922830>

19. Zhang, Q., Gao, Y., Zhang, J., Li, Y., Chen, J., Huang, R., Ma, G., Wang, L., Zhang, Y., Nie, K., & Wang, L. (2020). L-asparaginase exerts neuroprotective effects in an SH-SY5Y-A53T model of parkinson's disease by regulating glutamine metabolism. *Frontiers in Molecular Neuroscience*, 13. <https://doi.org/10.3389/fnmol.2020.563054>
20. Li, Q.-Q., Pan, S.-Y., Zhou, W., & Wang, S.-Q. (2021). [Effect of Competitive Antagonist of Transmembrane Glutamine Flux V-9302 on Apoptosis of Acute Myeloid Leukemia Cell Lines HL-60 and KG-1]. *Zhongguo Shi Yan Xue Ye Xue Za Zhi*, 685–689. <https://doi.org/10.19746/j.cnki.issn.1009-2137.2021.03.005>.
21. Mantena Rohit. (2021). Figure 1. Intracellular Mediated ROS Damage
22. Mantena Rohit. (2021). Figure 2. The Glutamine-Glutathione Conversion Process
23. Mantena Rohit. (2021). Figure 3: V-9302 Decreases Glutamine Uptake
24. Mantena Rohit. (2021). Figure 4: V-9302 Decreases Intracellular Glutamate Levels
25. Mantena Rohit. (2021). Figure 5: V-9302 Decreases Intracellular GSH Levels (ELISA)
26. Mantena Rohit. (2021). Figure 6: V-9302 Decreases Intracellular GSH Levels (Luminescence)
27. Mantena Rohit. (2021). Figure 7. The Glutamine-Glutathione Conversion Process – Step 1
28. Mantena Rohit. (2021). Figure 8. The Glutamine-Glutathione Conversion Process – Step 2
29. Mantena Rohit. (2021). Figure 9. The Glutamine-Glutathione Conversion Process – Step 3
30. Mantena Rohit. (2021). Figure 10: V-9302 Decreases Cell Proliferation
31. Mantena Rohit. (2021). Figure 11. V-9302 Decreases Cell Viability
32. Mantena Rohit. (2021). Figure 12. V-9302 Increases Cell Apoptosis
33. Mantena Rohit. (2021). Figure 13. V-9302 Increases Cell Apoptosis
34. Mantena Rohit. (2021). Figure 14: V-9302 Hampers Cell Metabolism
35. Mantena Rohit. (2021). Figure 15: V-9302 Increases  $\alpha$ -Synuclein levels
36. Mantena Rohit. (2021). Figure 16: V-9302 Increases ROS
37. Mantena Rohit. (2021). Figure 17. Glutamine vs  $\alpha$ -synuclein Regression Model
38. Mantena Rohit. (2021). Figure 18. Glutamate vs  $\alpha$ -synuclein Regression Model
39. Mantena Rohit. (2021). Figure 19. Glutathione vs  $\alpha$ -synuclein Regression Model

## Figures

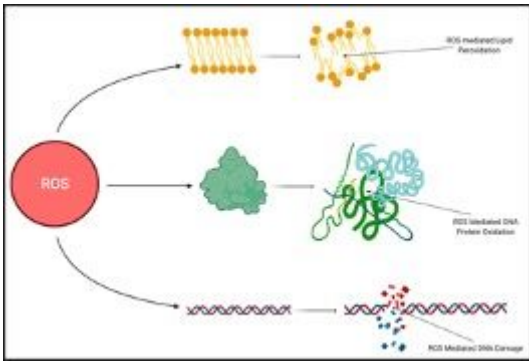


**Figure 1**

Intracellular Mediated ROS Damage. Generated by Author[21]

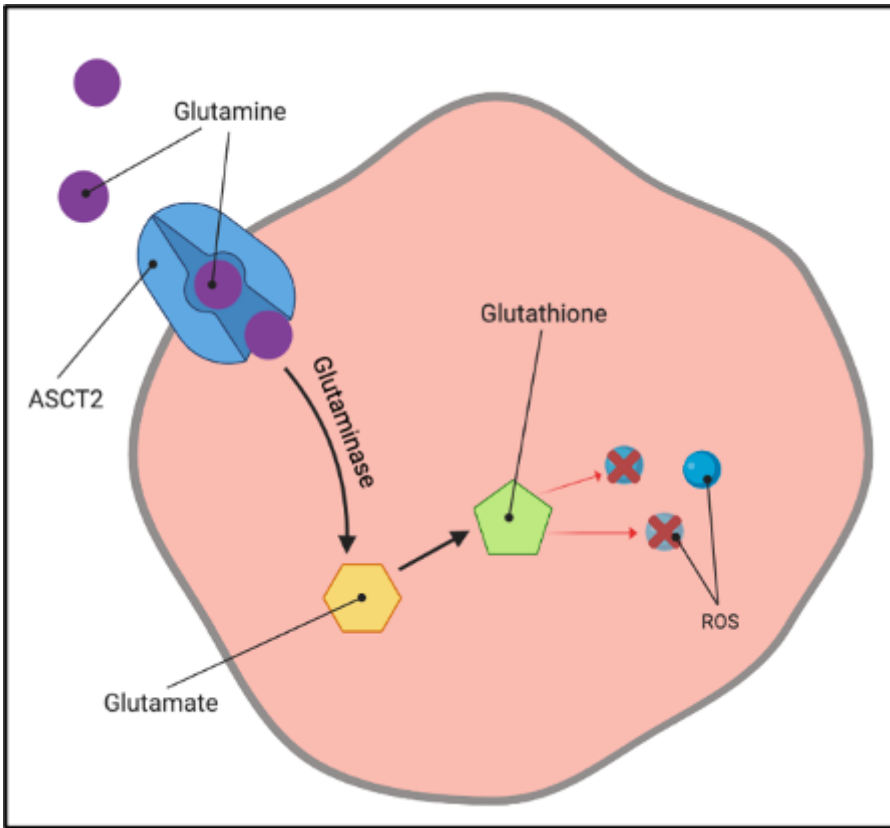


**Figure 2**

The Glutamine-Glutathione Conversion Process. Generated by Author[22]

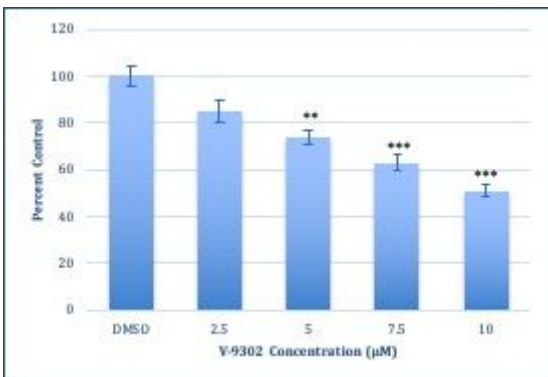


**Figure 3**

V-9302 Decreases Glutamine Uptake Generated by Author[23]. SH-SY5Y  $\alpha$ -synuclein-transfected cells were seeded at  $1.2 \times 10^5$  cells/mL density and treated with 0, 2.5, 5, 7.5, & 10  $\mu$ M of V-9302 dissolved in DMSO. Glutamine uptake was assessed with a glutamine uptake assay kit. Based on the data, there is a significant negative correlation between increased concentrations of V-9302 and glutamine uptake. Bars are means  $\pm$  STDEV (n=5). \* =  $p < 0.05$ , \*\* =  $p < 0.01$ , \*\*\* =  $p < 0.001$ .

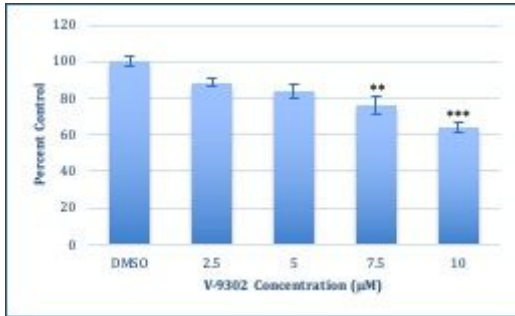


**Figure 4**

V-9302 Decreases Intracellular Glutamate Levels Generated by Author[24]. SH-SY5Y  $\alpha$ -synuclein-transfected cells were seeded at  $1.2 \times 10^5$  cells/mL density and treated with 0, 2.5, 5, 7.5, & 10  $\mu$ M of V-9302 dissolved in DMSO. Glutamine uptake was assessed with a glutamate levels assay kit. Based on the data, there is a significant negative correlation between increased concentrations of V-9302 and glutamate levels. Bars are means  $\pm$  STDEV (n=5). \* =  $p < 0.05$ , \*\* =  $p < 0.01$ , \*\*\* =  $p < 0.001$ .

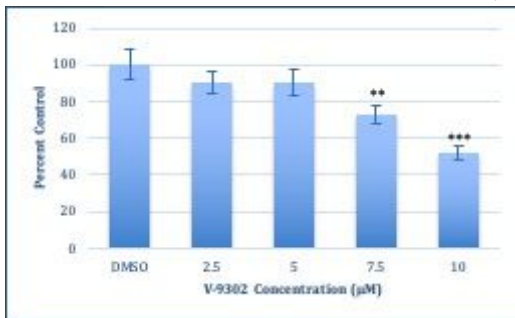


**Figure 5**

V-9302 Decreases Intracellular GSH Levels (ELISA) Generated by Author[25]. SH-SY5Y  $\alpha$ -synuclein-transfected cells were seeded at  $1.2 \times 10^5$  cells/mL density and treated with 0, 2.5, 5, 7.5, & 10  $\mu$ M of V-9302 dissolved in DMSO. Glutamine uptake was assessed with a two step, indirect ELISA. Based on the data, there is a significant negative correlation between increased concentrations of V-9302 and glutathione levels. Bars are means  $\pm$  STDEV (n=5). \* =  $p < 0.05$ , \*\* =  $p < 0.01$ , \*\*\* =  $p < 0.001$ .

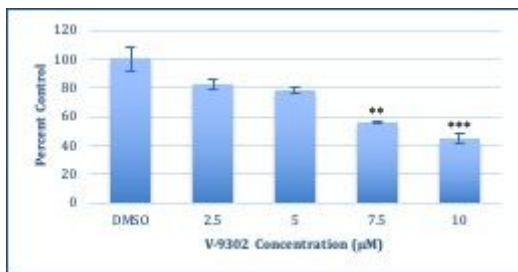


**Figure 6**

V-9302 Decreases Intracellular GSH Levels (Luminescence) Generated by Author[26]. SH-SY5Y  $\alpha$ -synuclein-transfected cells were seeded at  $1.2 \times 10^5$  cells/mL density and treated with 0, 2.5, 5, 7.5, & 10  $\mu$ M of V-9302 dissolved in DMSO. Glutamine uptake was assessed with a GSH-GLO assay kit. Based on the data, there is a significant negative correlation between increased concentrations of V-9302 and glutathione levels. Bars are means  $\pm$  STDEV (n=5). \* =  $p < 0.05$ , \*\* =  $p < 0.01$ , \*\*\* =  $p < 0.001$ .

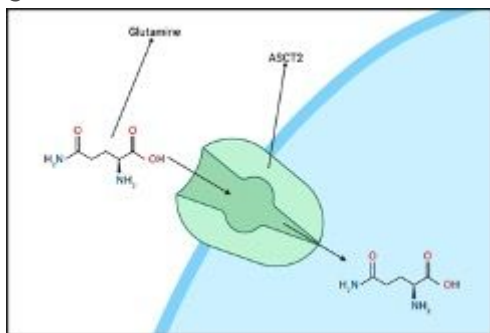


**Figure 7**

The Glutamine-Glutathione Conversion Process – Step 1. Generated by Author[27]

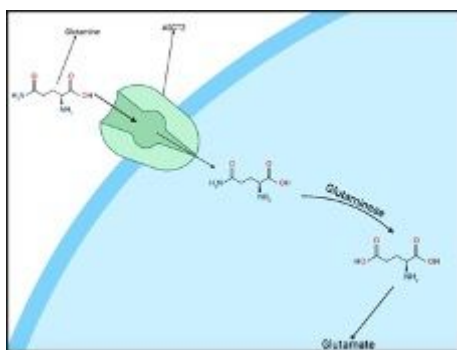


**Figure 8**

The Glutamine-Glutathione Conversion Process – Step 2. Generated by Author[28]

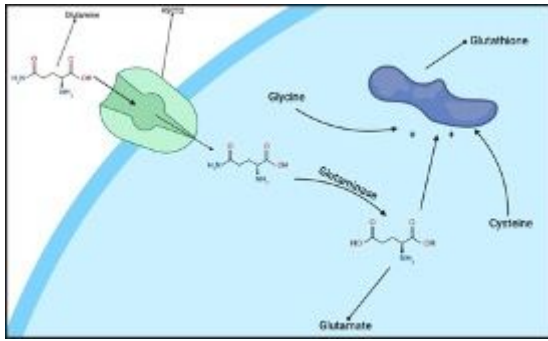


**Figure 9**

The Glutamine-Glutathione Conversion Process – Step 3. Generated by Author[29]

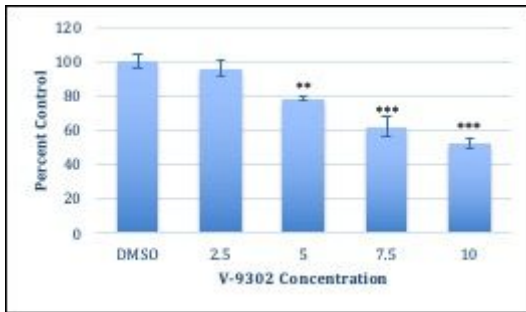


**Figure 10**

V-9302 Decreases Cell Proliferation Generated by Author[30]. SH-SY5Y  $\alpha$ -synuclein-transfected cells were seeded at  $1.2 \times 10^5$  cells/mL density and treated with 0, 2.5, 5, 7.5, & 10  $\mu$ M of V-9302 dissolved in DMSO. Cell proliferation was assessed by an MTS assay. Based on the data, there is a significant negative correlation between increased concentrations of V-9302 and cell proliferation. Bars are means  $\pm$  STDEV ( $n=5$ ). \* =  $p < 0.05$ , \*\* =  $p < 0.01$ , \*\*\* =  $p < 0.001$ .

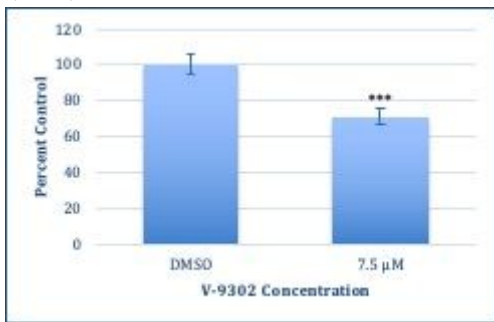


**Figure 11**

V-9302 Decreases Cell Viability Generated by Author[31]. SH-SY5Y  $\alpha$ -synuclein-transfected cells were treated with DMSO and 7.5  $\mu$ M V-9302 for 48 hours in t25 flasks. Then, cell viability was assessed. Based on the results, there is a significant drop in viability upon addition of V-9302. Bars are means  $\pm$  STDEV ( $n=5$ ). \* =  $p < 0.05$ , \*\* =  $p < 0.01$ , \*\*\* =  $p < 0.001$ .

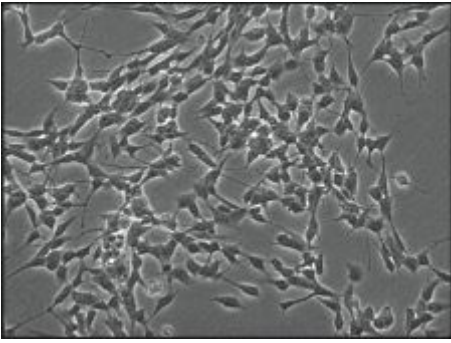


**Figure 12**

V-9302 Increases Cell Apoptosis. Generated by Author[32][33]. T25 flasks of SH-SY5Y  $\alpha$ -synuclein-transfected cells were cultured. a) Cells were treated with DMSO and cultured for 48 hours. Images were taken with an exposure of 15 ms and a magnification of 40x. b) Cells were treated with 7.5  $\mu$ M V-9302 and cultured for 48 hours. Images were taken with an exposure of 15 ms. When comparing the DMSO-treated cells to the V-9302 treated cells, there is far more neuronal branching and presence. Although the same contrast and exposure was applied, the V-9302 treated cells appear less refringent.

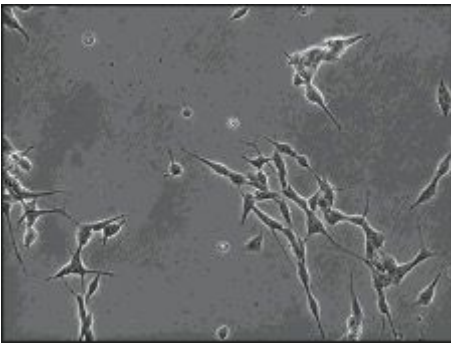


**Figure 13**

V-9302 Increases Cell Apoptosis. Generated by Author[32][33]. T25 flasks of SH-SY5Y  $\alpha$ -synuclein-transfected cells were cultured. a) Cells were treated with DMSO and cultured for 48 hours. Images were taken with an exposure of 15 ms and a magnification of 40x. b) Cells were treated with 7.5  $\mu$ M V-9302 and cultured for 48 hours. Images were taken with an exposure of 15 ms. When comparing the DMSO-treated cells to the V-9302 treated cells, there is far more neuronal branching and presence. Although the same contrast and exposure was applied, the V-9302 treated cells appear less refringent.

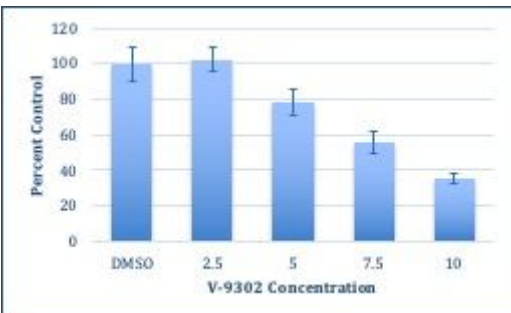


**Figure 14**

V-9302 Hampers Cell Metabolism Generated by Author[34]. SH-SY5Y  $\alpha$ -synuclein-transfected cells were seeded at  $1.2 \times 10^5$  cells/mL density and treated with 0, 2.5, 5, 7.5, & 10  $\mu$ M of V-9302 dissolved in DMSO. Cellular metabolism was assessed by measuring ATP production. Based on the data, there is a significant negative correlation between increased concentrations of V-9302 and ATP production. Bars are means  $\pm$  STDEV (n=5). \* =  $p < 0.05$ , \*\* =  $p < 0.01$ , \*\*\* =  $p < 0.001$ .

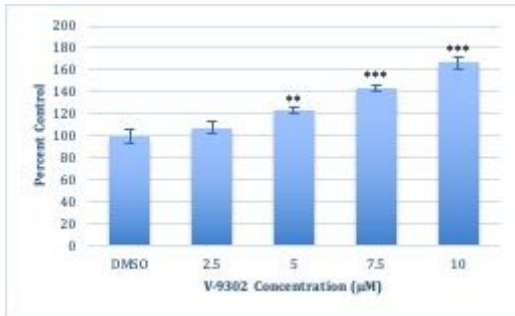


**Figure 15**

V-9302 Increases  $\alpha$ -Synuclein levels Generated by Author[35]. SH-SY5Y  $\alpha$ -synuclein-transfected cells were seeded at  $1.2 \times 10^5$  cells/mL density and treated with 0, 2.5, 5, 7.5, & 10  $\mu$ M of V-9302 dissolved in DMSO.  $\alpha$ -Synuclein levels were assessed with a two step, indirect ELISA. Based on the data, there is a significant positive correlation between increased concentrations of V-9302 and  $\alpha$ -Synuclein levels. Bars are means  $\pm$  STDEV (n=5). \* =  $p < 0.05$ , \*\* =  $p < 0.01$ , \*\*\* =  $p < 0.001$ .

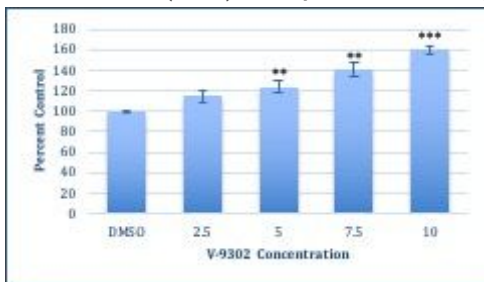


**Figure 16**

V-9302 Increases ROS Generated by Author[36]. SH-SY5Y  $\alpha$ -synuclein-transfected cells were seeded at  $1.2 \times 10^5$  cells/mL density and treated with 0, 2.5, 5, 7.5, & 10  $\mu$ M of V-9302 dissolved in DMSO. ROS levels were assessed with a ROS-GLO assay kit that used luminescence measurement to quantify intracellular ROS. Based on the data, there is a significant positive correlation between increased concentrations of V-9302 and intracellular ROS levels. Bars are means  $\pm$  STDEV (n=5). \* =  $p < 0.05$ , \*\* =  $p < 0.01$ , \*\*\* =  $p < 0.001$ .

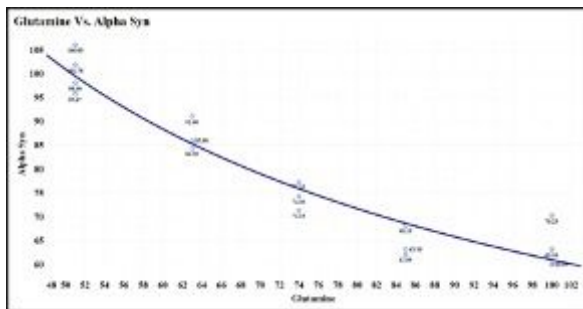


**Figure 17**

Glutamine vs  $\alpha$ -synuclein Regression Model Generated by Author[37]. A power regression model comparing glutamine levels with  $\alpha$ -synuclein levels was used to identify glutamine’s potential as a marker of  $\alpha$ -synuclein production. The equation of the power regression was  $y = [1732.2x]^{-0.727}$ ;  $R^2 = 0.9186$ . Based on the regression, the levels of glutamine and  $\alpha$ -synuclein have a strong negative correlation.

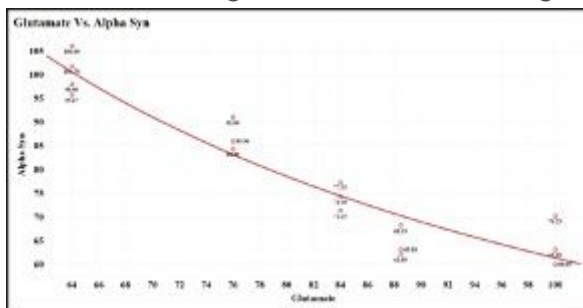


**Figure 18**

Glutamate vs  $\alpha$ -synuclein Regression Model Generated by Author[38]. A power regression model comparing glutamate levels with  $\alpha$ -synuclein levels was used to identify glutamate’s potential as a marker of  $\alpha$ -synuclein production. The equation of the power regression was  $y = [9999.2x]^{-1.106}$ ;  $R^2 = 0.8993$ . Based on the regression, the levels of glutamate and  $\alpha$ -synuclein have a strong negative correlation.

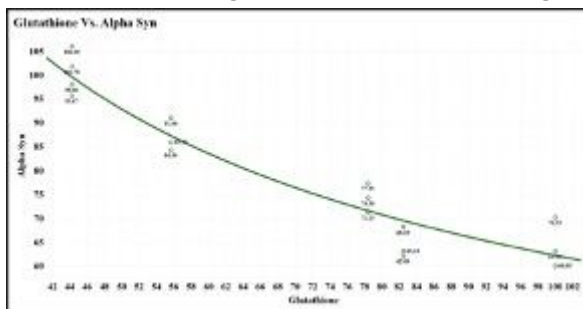


**Figure 19**

Glutathione vs  $\alpha$ -synuclein Regression Model Generated by Author[39]. A power regression model comparing glutathione levels with  $\alpha$ -synuclein levels was used to identify glutathione’s potential as a marker of  $\alpha$ -synuclein production. The equation of the power regression was  $y = [888.83x]^{-0.577}$ ;  $R^2 =$

0.9161. Based on the regression, the levels of glutathione and  $\alpha$ -synuclein have a strong negative correlation.